https://doi.org/10.5194/wes-2023-171
Preprint. Discussion started: 8 January 2024

eawe european academy of wind energy
Open Access WIND ENERGY SCIENCE DISCUSSIONS

An LES Model for Wind Farm-Induced Atmospheric Gravity Wave Effects Inside Conventionally Neutral Boundary Layers.

Sebastiano Stipa[1], Mehtab Ahmed Khan[2], Dries Allaerts[2], and Joshua Brinkerhoff[1]

[1]University of British Columbia, Okanagan Campus, CA
[2]Delft University of Technology, NL

Correspondence: Sebastiano Stipa (sebstipa@mail.ubc.ca)

Abstract. The interaction of large wind farm clusters with the thermally-stratified atmosphere has emerged as an important physical process that impacts the productivity of wind farms. Under stable conditions, this interaction triggers the creation of atmospheric gravity waves (AGWs) due to the vertical displacement of the boundary layer by the wind farm. AGWs induce horizontal pressure gradients within the boundary layer that alter the wind speed distribution within the farm, influencing both wind farm power generation and wake development. Additional factors, such as the growth of an internal boundary layer originating from the wind farm entrance and increased turbulence due to the wind turbines, further contribute to wake evolution. Recent studies have highlighted the considerable computational cost associated with simulating gravity wave effects within large eddy simulations (LES), as a significant portion of the free atmosphere must be resolved due to the large vertical spatial scales involved. Additionally, specialized boundary conditions are required to prevent wave reflections from contaminating the solution. In this study, we introduce a novel methodology to model the effects of AGWs without extending the LES computational domain into the free atmosphere. The proposed approach addresses the wave reflection problem inherently, eliminating the need for these specialized boundary conditions. We utilize the recently developed multi-scale coupled (MSC) model of Stipa et al. (2023b) to estimate the vertical boundary layer displacement triggered by the wind farm, and apply the deformation to the domain of an LES that extends only to the inversion layer. We validate our AGW modeling technique for two distinct free atmosphere stability conditions, comparing it to the traditional approach in which AGWs are fully resolved using a domain extending several kilometers into the free atmosphere. The proposed approach accurately captures AGW effects on the row-averaged thrust and power distribution of wind farms while demanding less than 15% of the computational resources compared to traditional methods. This can be further reduced in cases of conventionally neutral boundary layers, since there is no longer a need for solving the potential temperature equation. The developed approach is used to compare global blockage and pressure disturbances obtained from the simulated cases against a solution characterized by zero boundary layer displacement, which represents a limiting case of very strong free atmosphere stratification. Finally, we discuss the implications of making such "rigid-lid" approximation, instead of considering the full gravity wave solution, when predicting wind farm power.

https://doi.org/10.5194/wes-2023-171
Preprint. Discussion started: 8 January 2024

eawe european academy of wind energy
Open Access WIND ENERGY SCIENCE DISCUSSIONS

1 Introduction

Wind farms, especially those situated offshore, are increasing both in number and size, interacting with the atmosphere well beyond their physical boundaries. Such interactions play an important role both in the evolution of cluster wakes and on the amount of flow deceleration experienced upstream, also known as blockage. On the one hand, wind farm wake recovery is greatly influenced by surface stability within the atmospheric boundary layer (ABL). On the other hand, the stably stratified free atmosphere leads to the generation of atmospheric gravity waves (AGWs) when flow streamlines are vertically perturbed by the wind farm. These waves exist in the form of interface waves within the capping inversion layer and internal gravity waves aloft, introducing a pressure feedback mechanism at the wind farm scale that ultimately impacts the flow dynamics inside the ABL (Smith, 2010). In contrast to terrain-generated gravity waves (Smith, 1980, 2007), gravity waves triggered by wind farms yield smaller pressure and velocity perturbations inside the ABL as compared to turbulent fluctuations. This, combined with the extremely large spatial scales of AGWs and their dependence on the specific potential temperature structure, makes their observation and experimental measurement extremely difficult to achieve. Because of such complexities, AGWs have only been studied so far by means of high-fidelity models such as large eddy simulations (LES) or using linear gravity-wave theory (Nappo, 2012; Lin, 2007).

Using LES, the impact of gravity waves on the flow around wind farms has been subject of investigation by Allaerts and Meyers (2017); Lanzilao and Meyers (2022b); Stipa et al. (2023b); Lanzilao and Meyers (2023), who all assumed a conventionally neutral boundary layer (CNBL). This is characterized by a neutral stratification within the ABL, followed by a positive potential temperature jump $\Delta\theta$ across the inversion layer and by a stable free atmosphere with linear lapse rate γ aloft. The studies mentioned above showed that the presence of AGWs have two main implications, namely an adverse pressure gradient upwind the wind farm, which is responsible for global blockage, and a favorable pressure gradient inside the wind farm that is beneficial for wake recovery. Moreover, Centurelli et al. (2021) and Maas (2023) showed that LES results strongly differ from reduced-order wake models when thermal stratification is considered. To assess the impact of inversion height, strength and lapse rate on wind farm blockage, Lanzilao and Meyers (2023) conducted an LES parametric study, concluding that the overall effect of AGWs on wind farm operation is either beneficial or detrimental depending on the specific structure of the potential temperature profile. This result highlights the importance of including AGWs when modeling wind farms, both in high-fidelity and low-fidelity models.

An important aspect that emerges from the above studies, highlighted by Lanzilao and Meyers (2023), is that LES of wind farms including AGWs is a challenging endeavor. Firstly, they are rendered extremely computationally intense by the domain size that is required to resolve the large spatial scales associated with AGWs. Furthermore, special boundary conditions should be used to damp out AGWs before they reach the domain boundaries and reflect, contaminating the solution. In this regard, different approaches have been proposed in literature, such as radiation boundary conditions (Béland and Warn, 1975; Bennett, 1976), Rayleigh damping layers (Klemp and Lilly, 1978), or the fringe region technique (Inoue et al., 2014). The latter is a Rayleigh damping layer where the reference velocity used to compute the damping action depends on time, so that a concurrently resolved turbulent flow can be prescribed within the ABL while simultaneously damping wave reflections

https://doi.org/10.5194/wes-2023-171
Preprint. Discussion started: 8 January 2024

eawe european academy of wind energy
Open Access WIND ENERGY SCIENCE DISCUSSIONS

aloft. However, these approaches require *ad-hoc* tuning, usually accomplished by trial and error, which depends on the specific CNBL conditions and further raises computational costs. Some guidelines on how to choose the Rayleigh damping parameters were provided by Lanzilao and Meyers (2022a) and Klemp and Lilly (1978). Moreover, Lanzilao and Meyers (2022a) also noted that the fringe region itself may trigger spurious gravity waves, necessitating an additional layer in which horizontal advection of vertical momentum is suppressed to prevent these spurious perturbations to be transported downstream. Notably, many studies seem to agree that the Rayleigh damping layer located at the top should be larger than the expected vertical wavelength of the AGWs, estimated as $\lambda_z = 2\pi U_g/N$, where N is the Brunt-Väisälä frequency and U_g is the geostrophic wind (Klemp and Lilly, 1978; Allaerts and Meyers, 2017, 2018; Lanzilao and Meyers, 2022a). The same rule holds for the vertical height of free atmosphere to be included within the physical portion of the domain such that at least one vertical wavelength should be resolved.

The description of AGWs by means of reduced-order models was first achieved by Smith (1980, 2007) for the flow around terrain features, in what is referred to as the two-layer model (2LM). The 2LM exploits the theory for interacting gravity waves and boundary layers, later extended by Smith (2010) to wind farms immersed in CNBLs. Building on his work, Allaerts and Meyers (2019) developed the three-layer model (3LM), a substantial improvement of the 2LM characterized by extra features such as the Coriolis force, the additional wind farm layer that relaxes Smith's homogeneous vertical mixing assumption, and the wind farm/gravity wave coupling mechanism. Although the 3LM was the first study to incorporate AGW effects into predictions of the wind farm power losses, it lacked a local coupling between the mesoscale and turbine scales, failing to address the effects of gravity wave induced pressure gradients inside the wind farm and in the wake. Recently, Stipa et al. (2023b) proposed a new localized coupling strategy between the 3LM and conventional wake models, referred to as the multi-scale coupled model (MSC), capturing all features of the wind farm interaction with atmospheric gravity waves for CNBLs.

Under strong free atmosphere stability, lapse rate and inversion strength lose importance and the background pressure gradient is mainly determined by the height of the inversion. Such limiting case is commonly referred to as the rigid-lid approximation (Smith, 2023). Specifically, as the lid imposes zero vertical mass flux, the solution is characterized by an harmonic perturbation pressure that renders the flow horizontally divergence-free, with maximum and minimum pressure at the wind farm start and exit, respectively. In particular, the rigid-lid approximation maintains some properties of the full gravity wave solution, such as the presence of global blockage and flow acceleration within the wind farm. This, combined to its inherently simpler formulation than the full gravity wave solution, makes the rigid-lid approximation worth investigating for its potential use in engineering parametrizations.

In the present study, we propose a novel approach that models AGW effects within a wind farm LES while eliminating the computational burden associated with resolving internal and interfacial waves. In fact, while the proposed methodology uses LES below the inversion layer, AGWs in the free atmosphere and within the inversion layer are modeled through the MSC model (Stipa et al., 2023b). As a consequence, the developed approach only requires a vertical domain size that is equal to the height of the inversion layer. Moreover, if CNBLs are considered, the solution of a potential temperature transport equation is not required as the flow is neutral below the capping inversion. Finally, no damping regions are needed as the large-scale pressure gradient produced by AGWs is modeled without resolving the actual waves.

https://doi.org/10.5194/wes-2023-171
Preprint. Discussion started: 8 January 2024

eawe european academy of wind energy
Open Access WIND ENERGY SCIENCE DISCUSSIONS

The present paper is organized as follows. Section 2 describes the proposed LES methodology, pointing out its differences with respect to the conventional approach used to simulate the wind farm/gravity wave interaction. Section 3 describes the set-up of the LES cases used to verify the proposed methodology. Model verification is presented in Section 4, together with some considerations on the implications of using the rigid-lid approximation to model the inversion layer. Finally, Section 5 highlights the conclusions of the present study.

2 LES Methodology

For the LES simulations presented in this paper, we use the open-source finite volume code TOSCA (Toolbox fOr Stratified Convective Atmospheres) developed at the University of British Columbia and extensively validated in Stipa et al. (2023a). In order to distinguish between AGW-resolving simulations and the proposed approach, we first describe, in Section 2.1, the characteristics of a simulation that naturally resolves atmospheric gravity waves and their effects within the boundary layer. Then, in Section 2.2, we present the proposed modeling strategy with guidelines on its application. Only the turbulent part of the CNBL is included in the LES domain, while the steady-state solution in the free atmosphere is obtained from the MSC model.

2.1 AGW-Resolving Approach

As AGWs in the free atmosphere can only exist under stable conditions (Lin, 2007; Nappo, 2012), the present study focuses on CNBLs. This excludes those cases featuring a stable or unstable stratification within the ABL, which represent a subject for future investigation. Governing equations correspond to mass and momentum conservation for an incompressible flow with Coriolis forces and Boussinesq approximation for the buoyancy term. The latter is calculated using the modified density ρ_k, evaluated by solving a transport equation for the potential temperature. The exact form of the equations implemented in TOSCA and used in the present study is reported in Stipa et al. (2023a).

If one wishes to resolve AGW within LES, the simulation domain should extend to one or more wavelengths in each direction (Klemp and Lilly, 1978; Allaerts and Meyers, 2019; Stipa et al., 2023b; Lanzilao and Meyers, 2023). This greatly increases the computational cost, as AGWs are characterized by extremely large spatial scales, both vertically and horizontally. In addition, waves inherently reflect if they do not decay before reaching boundaries, requiring an even higher domain size or the use of damping regions where they are artificially damped before exiting the domain. Another source of contamination of the physical solution is represented by spurious gravity waves that are generated by damping regions themselves as they try to force physical perturbations to zero. This issue has been addressed by Lanzilao and Meyers (2022a), who developed the so called advection damping region, where horizontal advection of vertical velocity is brought to zero to prevent these spurious oscillations to be advected downstream. Furthermore, special care must be paid at the domain inlet in order to provide a time-dependent turbulent inflow to the simulation. For instance, it proves extremely difficult to damp out gravity waves and ensuring at the same time that turbulence is not distorted by the damping action if non-periodic boundary conditions are used in the streamwise direction. Moreover, two damping regions have to be applied in this case, namely at the inlet and outlet, respectively. Conversely, periodic

https://doi.org/10.5194/wes-2023-171
Preprint. Discussion started: 8 January 2024

eawe european academy of wind energy
Open Access WIND ENERGY SCIENCE DISCUSSIONS

boundary conditions allow to use the fringe region technique (Inoue et al., 2014), a damping layer in which the reference flow used to compute the damping source term is unsteady. This more easily allows to provide a realistic turbulent inflow while simultaneously damping wave reflections by using a single damping region located at the inlet (Stipa et al., 2023a) or at the outlet Lanzilao and Meyers (2022a,b).

These considerations highlight that the design of an LES simulation in which AGW effects are not altered by spurious or numerical phenomena is challenging. Such studies require trial and error to obtain a suitable size of the damping layers and their damping coefficients. Guidelines on selecting these quantities have only recently been provided by Lanzilao and Meyers (2022a). In light of such difficulties, a technique that eliminates the need for solving the governing equations in the free atmosphere and avoids damping regions will be a valuable tool to enable larger wind farm simulations at the same computational cost—or the same simulations at a reduced cost—while avoiding the *ad-hoc* tuning of the LES damping parameters.

2.2 AGW-Modeling Approach

As pointed out by Allaerts and Meyers (2017, 2018, 2019) and Lanzilao and Meyers (2022b), AGWs in the free atmosphere induce large-scale pressure gradients inside the ABL. The MSC model developed by Stipa et al. (2023b) is based on the concept that the effect of AGW on the wind farm is given by the change in mean velocity produced by this horizontally-varying pressure field, here referred as $p^\star$. Unfortunately, this idea cannot be directly applied to wind farm LES by prescribing $p^\star$ as a separate source term. In particular, for reasons that will be clarified later, the presence of the top boundary automatically prescribes a certain pressure gradient that satisfies mass and momentum conservation. In fact, the vertical streamline displacement η prescribed by the presence of the top boundary and the large-scale pressure field $p^\star$ cannot be imposed simultaneously, but are rather interdependent.

To explain the relationship between these two variables, we propose here a simple model obtained through a perturbation analysis applied to the depth-averaged linearized Navier-Stokes equations. This leads to consistent simplification of the equations proposed by Allaerts and Meyers (2019), while it still provides the required insight regarding the physics. In particular, we assume an infinitely wide wind farm in the spanwise direction, so that quantities can only change along the streamwise direction, i.e. $\partial/\partial y = 0$. Furthermore, the background flow is assumed to have a null mean spanwise component $V = 0$ (i.e. Coriolis forcing is neglected). The structure of the potential temperature profile is that of a CNBL characterized by lapse rate γ, inversion strength $\Delta\theta$ and inversion height H. The bulk velocity within the boundary layer and the geostrophic wind are referred to as U and U_g respectively. Similarly to Allaerts and Meyers (2019), the region below H is divided into two layers, namely the wind farm layer, characterized by a height H_1, and the upper layer, of depth $H - H_1$. The depth of the wind farm layer is chosen as twice the hub height, i.e. $H_1 = 2h_{\text{hub}}$. Finally, we assume that wind farm and upper layer are characterized by the same background velocity U, but at the same time admit different perturbation velocities u_1 and u_2. With the above

https://doi.org/10.5194/wes-2023-171
Preprint. Discussion started: 8 January 2024

eawe european academy of wind energy
Open Access WIND ENERGY SCIENCE DISCUSSIONS

simplifications, the 3LM equations derived by Allaerts and Meyers (2019) become

$$\begin{cases} U\dfrac{\partial u_1}{\partial x}+\dfrac{1}{\rho}\dfrac{\partial p^\star}{\partial x}=-\dfrac{C}{H_1}u_1-\dfrac{f_x}{H_1} \\ U\dfrac{\partial \eta_1}{\partial x}+H_1\dfrac{\partial u_1}{\partial x}=0 \end{cases} \tag{1}$$

and

$$\begin{cases} U\dfrac{\partial u_2}{\partial x}+\dfrac{1}{\rho}\dfrac{\partial p^\star}{\partial x}=0 \\ U\dfrac{\partial \eta_2}{\partial x}+H_2\dfrac{\partial u_2}{\partial x}=0, \end{cases} \tag{2}$$

where $C=2u^{*2}/U$. It should be noted that $\eta_1+\eta_2=\eta$, i.e. the total vertical displacement of the pliant surface initially located at H. This, at steady state, coincides with the flow streamline through H far upstream, and can be thought as the inversion layer displacement.

Rewriting the system in terms of η reads

$$\begin{cases} U\dfrac{\partial u_1}{\partial x}+\dfrac{1}{\rho}\dfrac{\partial p^\star}{\partial x}=-\dfrac{C}{H_1}u_1-\dfrac{f_x}{H_1} \\ U\dfrac{\partial u_2}{\partial x}+\dfrac{1}{\rho}\dfrac{\partial p^\star}{\partial x}=0 \\ U\dfrac{\partial \eta}{\partial x}+H_1\dfrac{\partial u_1}{\partial x}+H_2\dfrac{\partial u_2}{\partial x}=0, \end{cases} \tag{3}$$

To complete the system, we add an extra equation that relates the vertical inversion displacement to the pressure anomaly that will be felt inside the boundary layer due to the increase or decrease in weight of the air column overtopping a given x location. This can be expressed by means of linear theory (Nappo, 2012; Lin, 2007) as

$$\frac{1}{\rho}\hat{p}^\star=\Phi\hat{\eta}, \tag{4}$$

where Φ accounts for pressure anomalies generated by both the inversion layer displacement (surface waves) and the resulting motion aloft (internal waves). We refer to Smith (2010) and Allaerts and Meyers (2019) for the definition of such function; in this context it suffices to know that Φ contains all the physics related to AGWs and thermal stratification.

Equation (3) and Equation (4) form a fully determined system, which can be easily solved upon transformation into Fourier space. In particular, Equation (3) describes the flow physics below H, while Equation (4) refers to the flow in the free atmosphere. It can be observed that the pressure field $p^\star$ is the one that reconciles momentum and mass conservation inside the boundary layer with pressure anomalies due to overtopping density differences produced by a determined vertical displacement of the pliant surface at H. Specifically, η represents the coupling variable between the ABL and the free atmosphere, i.e. the neutral and stratified regions of the flow, respectively. Now, focusing only on the flow below H, i.e. on Equation (3), it is evident how the pressure gradient induced by AGWs—and its effects on the velocity—could be readily obtained without including thermal stratification if the inversion displacement η was somehow known and used to vertically deform the top boundary of the LES domain. Since a slip condition is usually applied to the top boundary, deforming this boundary alters the

https://doi.org/10.5194/wes-2023-171
Preprint. Discussion started: 8 January 2024

mean flow streamlines in a manner that is consistent with the inversion-layer displacement. Hence, AGWs given by different stability conditions can be easily modeled by suitably deforming the top boundary and then conducting the LES simulation of the turbulent part of the flow that is capped below the start of the stable flow region where the wind farm is located.

In the present study, we place the top boundary at the inversion center and use the full MSC model to compute η. Then, the vertical displacement is linearly distributed to the underlying cells, deforming the mesh before starting the simulation. Notably, the case where the top boundary is a flat surface corresponds to the rigid-lid limiting solution. In particular, while this differs from the actual solution with atmospheric gravity waves, it still allows to model both global blockage and flow acceleration within the wind farm produced by strong flow confinement inside the boundary layer. As a further consideration, since the overall pressure disturbance is fully determined by the inversion displacement, we note that any spatially-varying source term imposed in the form of a pressure gradient will not produce any effect on the simulation results, but rather change the significance of the pressure variable such that the original overall pressure disturbance is retained.

The developed approach is convenient for at least two reasons. First, it substantially reduces the computational cost by eliminating the need for damping regions and the requirement of a domain that is large enough to vertically resolve AGWs. Secondly, it eliminates the need to solve for a potential temperature transport equation as the flow below H is neutral in CNBLs. This condition is only violated very close to the top boundary, where discrepancies in turbulent fluctuations produced by the absence of stability and by the physical boundary are deemed acceptable as they happen away from the wind farm. Moreover, at the inversion height fluctuations are naturally close to zero, as this roughly coincides with the top of the boundary layer. A limitation of the method is that the accuracy of the large-scale pressure gradient produced by displacing the top boundary is dependent on the accuracy of the MSC model in predicting the overall physics of AGWs. Fortunately, Stipa et al. (2023b) showed that the pressure disturbance produced by the MSC model agrees well with a AGW-resolving wind farm LES simulations with different values of capping inversion strength.

3 Suite of Simulations

To verify the validity of the proposed approach, we use the two LES simulations available from Stipa et al. (2023b). These correspond to a subcritical and a supercritical regime of the CNBL, and are characterized by a domain size and damping region that is sufficient to resolve AGWs. For this reason, they are referred to as AGW-resolved cases in the present study. Each case is then compared to its AGW-modeled counterpart, where the technique proposed in Section 2.2 is applied. In addition, we used the developed modeling technique to simulate a case corresponding to the rigid-lid limiting solution, where the top boundary is not associated with any vertical displacement. Given its potential use in future engineering parametrizations, this allows to study the implications of such assumption in the flow solution and in the predicted wind farm power output.

3.1 AGW-Resolved Simulations

The subcritical and supercritical regimes of the AGW-resolved CNBL simulations are obtained by setting the inversion strength to 7.312 K and 4.895 K, respectively. Table 1 summarizes the remaining input parameters, namely the reference velocity u_{ref} at

https://doi.org/10.5194/wes-2023-171
Preprint. Discussion started: 8 January 2024

eawe european academy of wind energy
Open Access WIND ENERGY SCIENCE DISCUSSIONS

the reference height h_{ref} (chosen as the hub height), the reference potential temperature θ_0, the lapse rate γ, the inversion height H and the equivalent roughness length z_0. The Coriolis parameter f_c corresponds to a latitude of 41.33 deg. The simulated wind farm has a rectangular planform, with 20 rows and 5 columns organized in an aligned layout. The first row is located at $x = 0$, and extends from 300 m to 2700 m in the spanwise direction. This determines a lateral spacing of 600 m (4.76 D), while streamwise spacing is set to 630 m (5 D). Wind turbines correspond to the NREL 5-MW reference turbine, and are equipped with angular velocity and pitch controllers described in Jonkman et al. (2009). A very simple yaw controller is also added, which rotates wind turbines independently using a constant rotation speed of 0.5 deg/s when flow misalignment exceeds 1 deg. Flow angle is calculated by filtering the wind velocity at a sampling point located 1D upstream of the rotor center, using a time constant of 600 s. Turbines are modeled using the actuator disk model (ADM) described in Stipa et al. (2023a), while the tower and nacelle are not included in the simulation. The ADM force projection width is set to 18.75 m.

u_{ref} [m/s]	h_{ref} [m]	θ_0 [K]	Δh [m]	γ [K/km]	H [m]	f_c [1/s]	z_0 [m]
9.0	90	300	100	1	500	$9.6057 \cdot 10^{-5}$	0.05

Table 1. ABL parameters used for the finite wind farm simulation presented in this section

The AGW-resolved simulations employ the hybrid off-line/concurrent precursor method described in Stipa et al. (2023a). For the off-line precursors, the Rampanelli and Zardi (2004) model is used to initialize the potential temperature profile, where we take H as the center of the capping inversion layer. Both off-line precursors are advanced in time for 10^5 s, after which data are averaged for $2 \cdot 10^4$ s. Their domain size is of 6 km $\times$ 3 km $\times$ 1 km in the streamwise, spanwise, and vertical directions respectively. The off-line precursor mesh has a horizontal resolution of 15 m, while in the vertical direction it is graded equally as the concurrent precursor and successor simulations, described later. A driving pressure controller with geostrophic damping is used to fix the average velocity at h_{ref} while a potential temperature controller is used to fix the average potential temperature profile throughout the simulation (both controllers and geostrophic damping use the same settings reported in Stipa et al., 2023a). The concurrent precursor method requires periodic boundary conditions combined with a single fringe region, which we locate at the domain inlet. This allows a time-varying turbulent flow to be produced while eliminating the reintroduction of the wind farm wake at the inlet by the periodic boundary and damping gravity wave reflections. At the upper boundary, we use a Rayleigh damping layer with a thickness of 12 km, i.e. slightly more than one expected vertical wavelength (this parameter can be calculated as $\lambda_z = 2\pi U_g/N$, where N is the Brunt-Väisälä frequency and U_g is the geostrophic wind). Lateral boundaries are periodic, implying that gravity waves induced by the wind farm will interact with their periodic images. This dictates that the domain must be sufficiently large for these interactions to happen far from the wind turbines. Moreover, we use the advection damping technique developed by Lanzilao and Meyers (2022a) to ensure that interactions between fringe-generated and physical gravity waves are not advected downstream but instead remain trapped inside the advection damping region. Specifically, we set the Rayleigh damping coefficient to $\nu_{RDL} = 0.05$ s^{-1} and the fringe damping coefficient to $\nu_{FR} = 0.03$ s^{-1}. The damping functions are identical to Lanzilao and Meyers (2022a) and their parameters are reported in Table 2.

https://doi.org/10.5194/wes-2023-171
Preprint. Discussion started: 8 January 2024

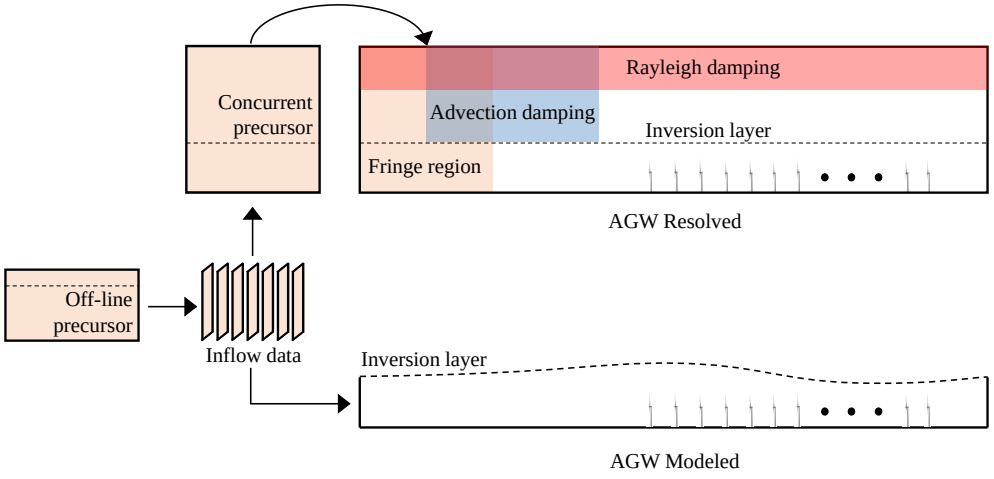

Figure 1. Methodological sketch comparing the AGW-resolved method (top) and the AGW modeled approach (bottom).

x_s [km]	x_e [km]	Δ_s [km]	Δ_e [km]
-20	-15	1	1

(a) Fringe region parameters.

x_s [km]	x_e [km]	Δ_s [km]	Δ_e [km]
-18	-11	1	1

(b) Advection damping region parameters.

Table 2. Fringe and advection damping region information.

The domain size of the AGW-resolved cases is 40 km $\times$ 21 km $\times$ 28 km in the streamwise, spanwise and vertical direction respectively, discretized with 1554 $\times$ 1194 $\times$ 345 cells. All directions are graded to reach a mesh resolution of 30 m $\times$ 12.5 m $\times$ 10 m around the wind farm. The concurrent precursor mesh coincides with the portion of the successor domain located inside the fringe region. As a consequence, it extends for 5 km $\times$ 21 km $\times$ 28 km. Here, the mesh resolution in the streamwise direction is 15 m, while in the spanwise and vertical directions it is identical to the successor mesh. Additional details of the AGW-resolved simulations are provided in Stipa et al. (2023b).

3.2 AGW-Modeled Simulations

The AGW-modeled simulations feature the same horizontal domain size and discretization as the AGW-resolving cases. Conversely, the vertical domain size is set to 500 m so that the top boundary is coincident with the unperturbed inversion height. Moreover, as the fringe region, Rayleigh and advection damping layers are not required, inlet-outlet boundary conditions are used along x. Specifically, we conducted two additional off-line precursor simulations corresponding to the subcritical and supercritical conditions. These are first run for 10^5 s, after which data are averaged for $4 \cdot 10^4$ s and inflow sections are saved at each iteration to be used as inlet boundary conditions in the wind farm successors. These additional precursor cases are characterized by an enlarged spanwise domain size of 21 km – coincident with the successor cases – to avoid the spanwise

https://doi.org/10.5194/wes-2023-171
Preprint. Discussion started: 8 January 2024

eawe european academy of wind energy
Open Access WIND ENERGY SCIENCE DISCUSSIONS

periodization of the inflow data that used by Stipa et al. (2023b) in the AGW-resolved cases. In fact, as reported by the same authors, this led to turbulent streaks that slowed down the convergence of turbulence statistics. Moreover, we applied a spanwise shift velocity of 1 m/s to the inflow data in the successor simulations, with the objective of enhancing statistics convergence. Specifically, instead of being added to the inflow velocity field, such shift velocity is used to physically move the inflow data along the spanwise direction so that the average wind direction remains unaffected. The inflow data is then mapped at the successor inlet patch by means of bi-linear interpolation, further interpolating at the desired time value from the two closest available times. AGW-modeled simulations are progressed in time for $4 \cdot 10^4$ s, using the entire inflow database. As our method does not require the definition of a potential temperature field, nor the solution of the corresponding equation, we used the velocity inflow data of the subcritical case to prescribe an inlet for the rigid lid simulation. A qualitative comparison between the AGW-resolved and AGW-modeled methodologies is reported in Figure 1.

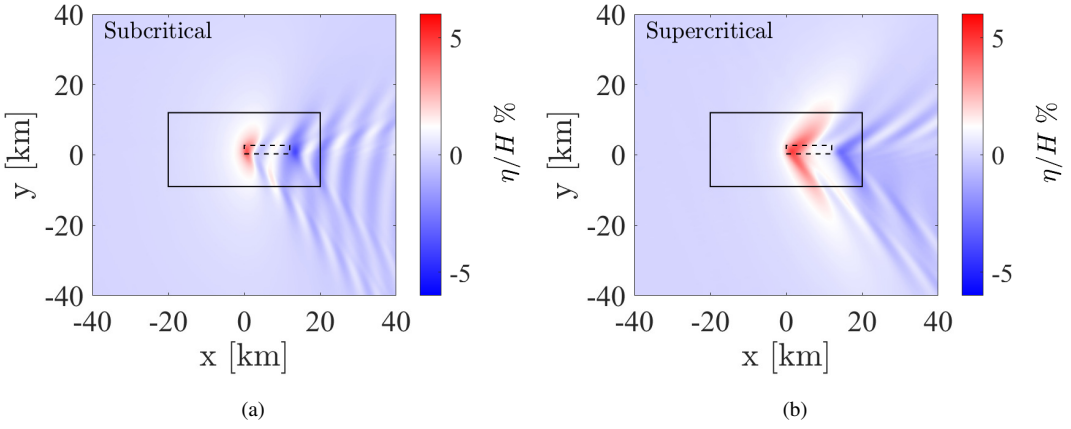

Figure 2. Inversion displacement as a percentage of the boundary layer height for (a): subcritical case and (b): supercritical case. The LES domain is identified by the continuous rectangle, while the wind farm is represented by the dashed rectangle.

Finally, the simulation setup for the AGW-modeled cases is complete upon providing the inversion layer displacement that is necessary to vertically deform the top boundary. As previously mentioned, this is calculated using the MSC model. As the model's input parameters are detailed in Stipa et al. (2023b), we only show the resulting inversion displacement corresponding to the subcritical and supercritical cases in Figure 2.

4 Results

The proposed modeling approach has two main advantages. First, it allows to cut down the computational cost associated with including AGW effects in wind farm simulations, by requiring a domain that only extends to the capping inversion layer. For the cases presented in this manuscript, the AGW-modeling technique requires a domain that is more than 85% smaller

https://doi.org/10.5194/wes-2023-171
Preprint. Discussion started: 8 January 2024

eawe european academy of wind energy
Open Access WIND ENERGY SCIENCE DISCUSSIONS

compared to the AGW-resolving approach. Secondly, it does not require numerical artifacts aimed at damping gravity waves reflections at the domain boundaries, as these waves are not physically resolved by the simulation.

In Section 4.1, the accuracy of the proposed AGW-modeling method is verified against AGW-resolving simulations corresponding to Stipa et al. (2023b), for both subcritical and supercritical conditions. Then, in Section 4.2, we investigate the implications of employing the rigid-lid approximation (Smith, 2023) in terms of our ability to capture global blockage effects. The latter completely neglects free atmosphere stability and treats the inversion layer as a rigid lid that cannot be deformed. As a consequence the resulting horizontal pressure gradient solely responds to the requirement of mass conservation inside the boundary layer.

In the following analysis, time averaging of the simulation results was performed for $15,000$ s following the establishment of a statistically-steady flow field. Moreover, since the AGW-modeled cases used different precursor time histories from the AGW-resolved counterparts, the start of the time averaging window was shifted in time until the row-averaged freestream velocity at the first turbine row matched those from the corresponding AGW-resolved simulations. This procedure allows to compare the two approaches eliminating any bias in freestream wind speed produced by the different large-scale turbulent structures in the two cases. More details on this procedure and on its motivation are reported in Appendix A.

4.1 Model Verification

Global blockage can be seen as the wind responding to the pressure gradient induced by the mean vertical displacement of the boundary layer due to the vertical perturbation triggered by the wind farm and the corrective response provided by buoyancy forces. Specifically, the induced perturbation pressure field is heterogeneous in space and features an unfavorable pressure gradient region upstream of the farm and a favorable region that extends through most of the cluster. Downstream and around the wind farm, the perturbation pressure field is strongly dependent on the strength of the inversion, the free atmosphere lapse rate, and the geostrophic wind.

In light of the critical role played by the perturbation pressure field, we first compare the mean pressure variations resulting from the AGW-modeled approach with those obtained by resolving gravity waves in the free atmosphere. Figure 3 plots the streamwise distribution of pressure perturbation, spanwise-averaged over the wind farm width in the upper layer (from $2h_{\mathrm{hub}}$ to H), for both the subcritical and supercritical cases. For completeness, we also show the pressure variation resulting from the MSC model. In both atmospheric cases, the AGW-modeled and the AGW-resolved approach predict almost the same pressure perturbation distribution. This, as explained in Section 2.2, is a function of the imposed vertical boundary layer displacement for the AGW-modeled simulations, while it naturally arises from the free atmosphere solution in the AGW-resolved approach. As previously reported by Stipa et al., 2023b, data are also in good agreement with results from the MSC model. Subcritical conditions produce larger pressure gradients if compared to the supercritical ABL state, both unfavorable upstream and favorable inside the wind farm. Moreover, lee waves can be observed in subcritical conditions (also visible in Figure 2), which induce pressure oscillations on a wavelength that is smaller than the wind farm length. These waves lead to oscillations in the background velocity field that yield power variations throughout the wind farm as well as an intermittent wake recovery (Stipa et al., 2023b). In both atmospheric states, the largest difference between the AGW-resolved simulations

https://doi.org/10.5194/wes-2023-171
Preprint. Discussion started: 8 January 2024

eawe european academy of wind energy
Open Access WIND ENERGY SCIENCE DISCUSSIONS

and the AGW-modeled and MSC results is near the domain exit. In our opinion, this is because the AGW-resolved simulations employ a fringe region at the domain inlet in which a source term is applied that removes the wind farm wake by forcing the flow to adhere to the concurrent-precursor solution by the fringe exit. In so doing, the fringe region modifies the momentum balance, altering the pressure field both inside and immediately upwind of the fringe region, which coincides with the domain exit in Figure 3 owing to the periodic boundary conditions.

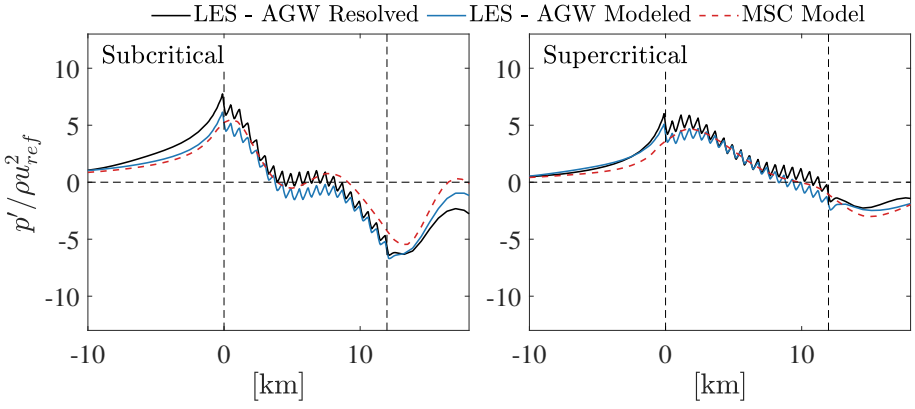

Figure 3. Time- and spanwise-averaged pressure perturbation between $y = 0$ and $y = 3000$ m. For completeness, we also report data from the MSC model, in dashed red.

In Figure 4, we report the streamwise evolution of velocity, averaged over time and over the wind farm width, for both the subcritical and supercritical ABL states. Overall, results from using the AGW-modeled and AGW-resolved methods are in good agreement with each other, indicating that the proposed methodology is able to capture not only blockage, but also the entirety of gravity wave effects on the ABL flow. Velocity reductions extending several kilometers upstream of the wind farm can be observed in both cases, indicating the presence of global blockage. Moreover, the mean velocity deficit in the wind farm wake is captured equivalently between both cases, where the effect of gravity-wave induced pressure gradients on promoting wake recovery can be observed, especially for the subcritical case. (Stipa et al., 2023a).

https://doi.org/10.5194/wes-2023-171
Preprint. Discussion started: 8 January 2024

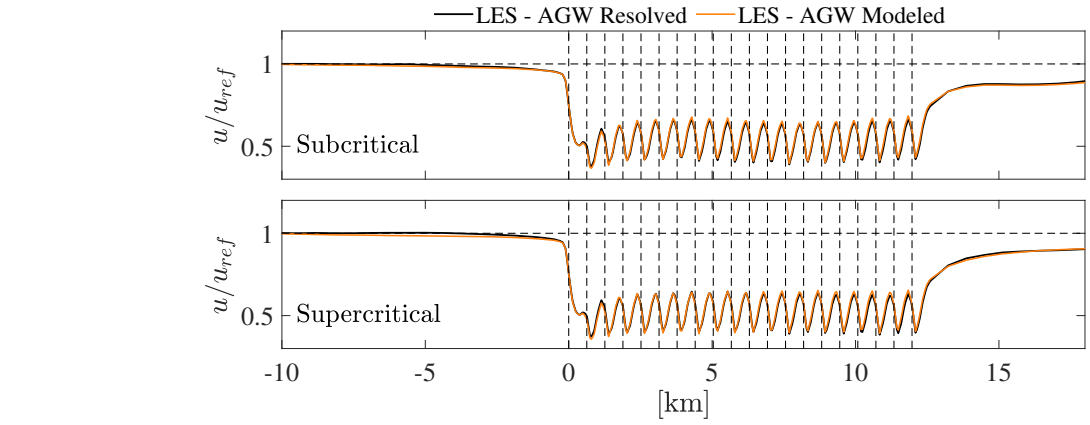

Figure 4. Time and spanwise averaged velocity between $y = 0$ and $y = 3000$ m.

In order to verify the accuracy of the proposed method in capturing the trend turbine thrust and power along the wind farm length, the time and row-averaged thrust and power at each wind farm row is plotted in Figure 5 for both the subcritical and supercritical cases. The effect of lee waves aloft in the subcritical state can be appreciated by looking at the large scale oscillations in thrust and power throughout the wind farm. Moreover, the weaker favorable pressure gradient that characterizes supercritical conditions implies lower power towards the wind farm exit. Conversely, the subcritical state is affected by a stronger unfavorable pressure gradient upwind, leading to increased blockage effects. In general, increased blockage also leads to a more favorable pressure gradient within the wind farm but, as demonstrated by Lanzilao and Meyers (2023), whether the net result is beneficial or detrimental depends on the specific conditions. Overall, the proposed AGW-modeling approach captures the effects of gravity waves on the wind farm thrust and power (see Table 3), which is arguably the most important information obtained from a wind farm LES.

	P [MW] AGW-R	P [MW] AGW-M
subcritical	135.0	139.5
supercritical	133.5	133.3

Table 3. Overall wind farm power obtained from LES simulations in subcritical and supercritical conditions using the AGW-resolving (AGW-R) and AGW-modeling (AGW-M) techniques.

https://doi.org/10.5194/wes-2023-171
Preprint. Discussion started: 8 January 2024

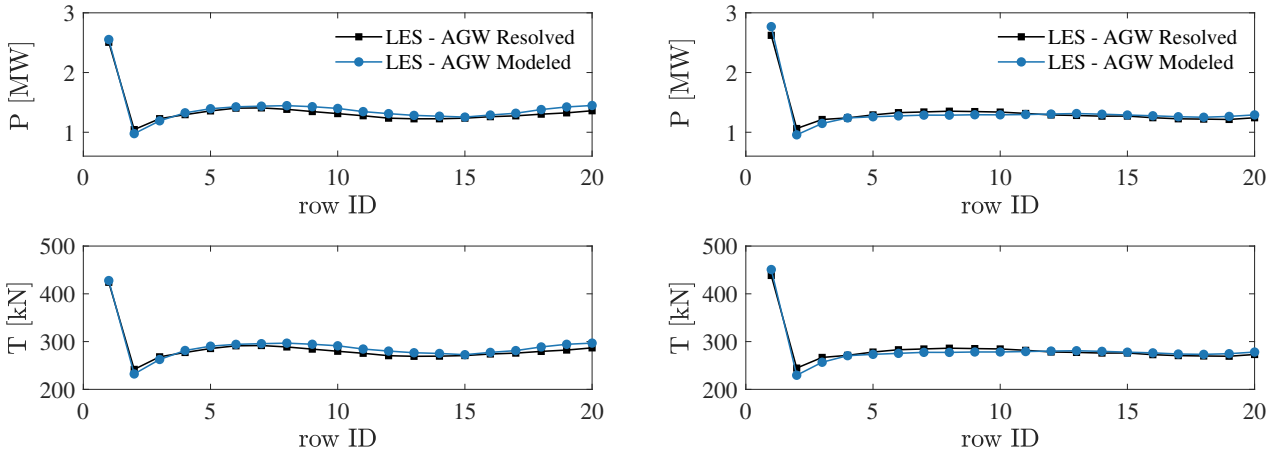

(a) Subcritical (b) Supercritical

Figure 5. Comparison of row-averaged thrust and power distributions for wind farm (a) subcritical and (b) supercritical cases.

4.2 Rigid Lid Approximation

In the present section, we leverage the proposed methodology to assess the implications of the rigid-lid approximation in evaluating global blockage effects. Although this is certainly attractive from an engineering standpoint, as it allows for a simpler simulation, it fails to account for gravity waves. The impact of this omission on the global blockage is therefore assessed.

To enforce the rigid-lid approximation within LES, we employ the AGW-modeling technique where no vertical displacement of the top boundary is applied. Figure 6 shows streamwise distributions of velocity and pressure, averaged in time and over the width of the wind farm. In particular, we compare the subcritical, supercritical and rigid-lid cases, all obtained using the AGW-modeling approach. A close up view of the blockage region within 1 km upstream of the wind farm is also reported. First, by looking at the pressure gradient, it can be noticed how each case is characterized by an anti-symmetric pressure distribution, with maximum and minimum at the wind farm start and exit, respectively. Moreover, the rigid-lid approximation is characterized by the smallest values of favorable and unfavorable pressure gradients upstream and inside the wind farm, respectively. As a consequence, while the rigid-lid approximation features global blockage, it is less pronounced than both subcritical or supercritical conditions. Regarding wake recovery, results from the rigid-lid case exhibits the highest deficit. Overall, while it is clear that the rigid-lid approximation cannot track gravity-wave induced effects, our results indicate that flow confinement is responsible for a certain (lesser) extent of the global blockage.

https://doi.org/10.5194/wes-2023-171
Preprint. Discussion started: 8 January 2024

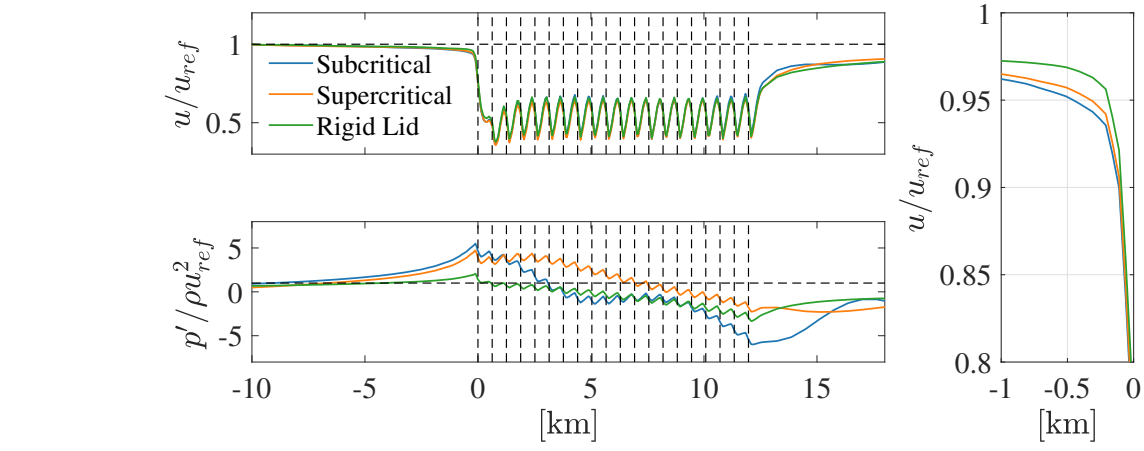

Figure 6. Comparison between subcritical, supercritical and rigid lid limiting solution. Data correspond to the AGW modeled simulations.

In particular, referring to the time and row-averaged power distributions depicted in Figure 7, it can be stated that, for the simulated conditions, results obtained using the rigid-lid approximation are not far from the subcritical and supercritical figures. Again, while wind farm gravity wave interaction is completely missing, overall wind farm power from the rigid-lid case agrees with the cases that include the effect of gravity waves.

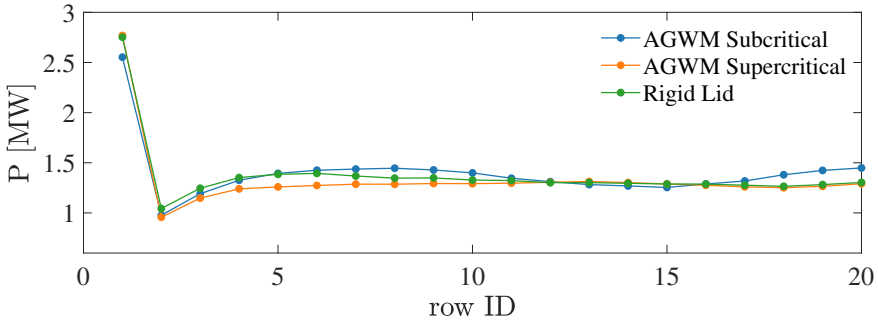

Figure 7. Row-averaged power from the subcritical, supercritical and rigid lid limiting solution. Data relative to the subcritical and supercritical conditions correspond to the AGW modeled simulations.

To further investigate this aspect, we used the MSC model to run a parametric analysis in which lapse rate and inversion jump are systematically varied from 1 to 10 K/km and 0 to 10 K, respectively. For each of these atmospheric states, we compute the quantity $(P_{RL} - P_{MSC})/P_{MSC}$, where P_{RL} and P_{MSC} are the values of total wind farm power obtained using the rigid-lid assumption within the MSC and the full MSC calculation that accounts for gravity waves, respectively.

https://doi.org/10.5194/wes-2023-171
Preprint. Discussion started: 8 January 2024

eawe european academy of wind energy
Open Access WIND ENERGY SCIENCE DISCUSSIONS

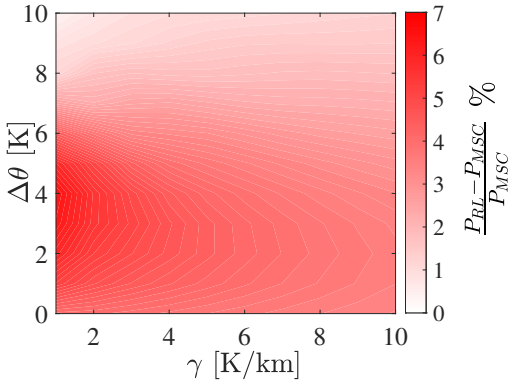

Figure 8. Error relative to the AGW solution on wind farm power produced by the rigid-lid approximation, as predicted by the MSC model.

Our results, reported in Figure 8, show that the full gravity wave solution approaches the rigid-lid approximation for high values of inversion strength and free atmosphere lapse rate. This is consistent with the grounds upon which the approximation is based. Moreover, it can be noticed how the approximation always over-predicts wind farm power, with greater errors (around 7%) observed for supercritical conditions ($\Delta\theta$ approximately less than 6 K for this specific background wind profile) and low values of the free atmosphere lapse rate. This trend is generally confirmed by the LES results, and it is reported in Table 4. Specifically, the rigid-lid case under-estimates power by 1.5% if compared to the subcritical case, while power is overestimated by 3% with respect to the supercritical case. Finally, in light of what stated above, the error is expected to reduce if higher values of the free atmosphere lapse rate are considered.

	P [MW]	err [%]
subcritical	139.5	-1.5
supercritical	133.3	3.0
rigid-lid	137.4	

Table 4. Overall wind farm power obtained from LES simulations in subcritical and supercritical conditions, as well as employing the rigid-lid approximation. The error of the latter with respect to the first two cases is also reported.

5 Conclusions

In this study, we introduced an approach that allows the effects of wind farm self-induced atmospheric gravity waves to be modeled without actually resolving these waves in the simulation. The proposed method couples the LES solution below the inversion layer with the MSC model developed by Stipa et al., 2023b. Specifically, the vertical perturbation to the inversion layer produced by the wind turbines, evaluated with the MSC model, is used to vertically deform the top boundary in the LES domain. Since prescribing the inversion displacement automatically establishes the pressure field below, the resulting LES

https://doi.org/10.5194/wes-2023-171
Preprint. Discussion started: 8 January 2024

eawe european academy of wind energy
Open Access WIND ENERGY SCIENCE DISCUSSIONS

velocity field contains the influence of gravity waves. If conventionally neutral boundary layers (CNBLs) are simulated, temperature transport becomes irrelevant as the flow is neutrally stratified inside the domain. Atmospheric gravity wave feedback with the wind farm is provided by running the MSC model with multiple coupling iterations. The proposed method implies a computational domain that only requires 15% of the cells used in the conventional AGW-resolved method. Moreover, simultaneous solution of a concurrent-precursor and the use of a fringe region are not required, as there are no gravity waves in the domain. More generally, tedious and complex measures to avoid spurious gravity waves reflections, such as the Rayleigh damping layer and the fringe region, are no longer required.

The proposed approach has been verified against the LES simulations conducted in Stipa et al., 2023b. These are characterized by a set-up that allows to resolve gravity waves, and correspond to subcritical and supercritical regimes of interfacial waves within the inversion layer. Our results show that the proposed method is able to accurately capture the impact of gravity waves on pressure and velocity, including blockage effects. Moreover, the row-averaged thrust and power distributions are in good agreement with that of the AGW-resolved approach.

Overall, our analysis shows that the proposed AGW-modeled method allows to model the impact of atmospheric gravity waves on wind farm performance at a reduced computational cost and with great accuracy. A drawback of the approach is that its performance depends on how accurately the MSC model captures the displacement of the inversion layer. Moreover, the MSC model is currently limited to stationary and conventionally neutral boundary layers. For this reason, future work aims at including internal stability and time-dependency into the MSC model, enabling the AGW-modeling method to simulate evolving and arbitrary ABL inflow conditions within LES at a low computational cost.

Furthermore, we used the AGW-modeling method to study the implications of adopting the rigid-lid approximation (Smith, 2023). The latter neglects the inversion layer displacement produced by gravity waves by only considering the effects of flow confinement imposed by the unperturbed inversion layer height. While details due to wind farm gravity waves are expectedly absent, flow confinement alone still yields global wind farm blockage, and leads to surprisingly small errors (less than 3%) in overall wind farm power when compared to the full gravity wave solution. To this end, the MSC model has been used to systematically map the error in global wind farm power produced by the rigid-lid approximation with different values of inversion strength and free atmosphere stratification. The approximation performs worse for supercritical interface wave regimes and low values of the lapse rate ($4-7$ % difference), while the error reduces with increasing free atmosphere stability.

https://doi.org/10.5194/wes-2023-171
Preprint. Discussion started: 8 January 2024

eawe european academy of wind energy
Open Access WIND ENERGY SCIENCE DISCUSSIONS

Appendix A: Effect of Atmospheric Turbulence on Thrust and Power Averages

As mentioned in Section 3, although precursor simulations for the AGW-resolved and AGW-modeled cases shared the same inputs parameters, they run on domains of different size. As a consequence, although simulations corresponding to the same CNBL conditions produce identical horizontally-averaged fields, they also result in different realizations of their time-resolved turbulent field. While this is not a problem for the small eddies, large turbulent structures may change the freestream velocity obtained by averaging over a time window that is comparable with their size. This is evident from Figure A1b, where we report the instantaneous wind, averaged among the first row turbines, for the AGW-resolved and AGW-modeled approaches corresponding to both subcritical and supercritical conditions. When averaging time histories of e.g. turbine power or thrust, this effect could introduce a consistent bias as these quantities depend on the cube and square of velocity, respectively. Unfortunately, for a time window of the order of the one used in the present study ($15,000$ s), such effect introduces a variability in wind farm thrust and power that is comparable with the effect if blockage. This is shown in Figure A1a, where we report the time history of the velocity sampled at the domain inlet and close to the wind turbine located first row center, for both the subcritical and supercritical AGW-modeled simulations. As can be noticed, even though $15,000$ s can be considered a large averaging window, the variations in average velocity obtained by hypothetically shifting this average in time are expected to be comparable with, if not bigger than, global blockage effects.

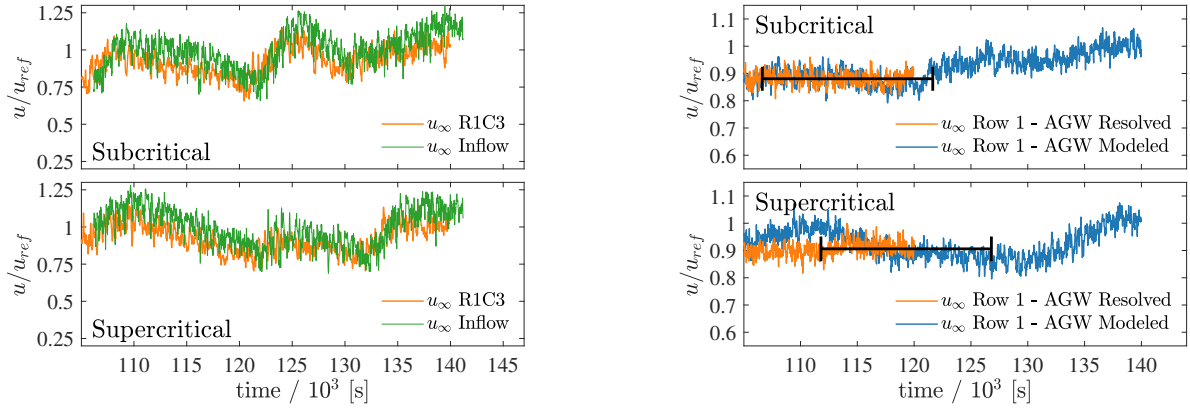

(a) (b)

Figure A1. (a): hub-height wind speed at the domain inlet (green) and as sampled by the wind turbine located in the middle of the first row (orange). Data correspond to the subcritical and supercritical AGW-modeled simulations. (b): wind speed averaged among the first row wind turbines for the AGW-resolved (orange) and AGW-modeled (blue) cases. Data correspond to the subcritical and supercritical cases. The black bar indicates the time window used to average turbine data in the AGW-modeled simulations.

For this reason, when comparing turbine power and thrust between AGW-modeled and AGW-resolved methods under the same CNBL conditions, we chose the averaging window for the former case as follows. First, we ensure that the same window is used for both cases, i.e. $15,000$ s, corresponding to the entirety of the data available from the AGW-resolved analyses. Then,

https://doi.org/10.5194/wes-2023-171
Preprint. Discussion started: 8 January 2024

eawe european academy of wind energy
Open Access WIND ENERGY SCIENCE DISCUSSIONS

we shift the averaging window in the AGW-modeled cases until the freestream velocity averaged among the first row turbines matches the same quantity obtained from the AGW-resolved simulation. The averaging window resulting from this approach is reported in black in Figure A1b, for both subcritical and supercritical conditions. Finally, turbine thrust and power from the AGW-modeled cases are averaged over this window, ensuring that the wind farm sees the same inflow velocity in the two cases. Regarding flow variables, these are always averaged throughout the entire simulation, i.e. from $105,000$ to $120,000$ s for the AGW-resolved and from $105,000$ s to $140,000$ s for the AGW-modeled cases. While it is true that the approach described above likely forces the first row average power to match between AGW-resolved and AGW-modeled cases characterized by the same CNBL conditions, it allows thrust and power distributions to vary in the remaining rows.

https://doi.org/10.5194/wes-2023-171
Preprint. Discussion started: 8 January 2024

Code availability. TOSCA is available at https://github.com/sebastipa/TOSCA

Author contributions. Conceptualization, S.S, M.A.K., D.A., J.B.; methodology, S.S., M.A.K.; software, S.S; validation, S.S.; formal analysis, S.S.; investigation, S.S., M.A.K; computational resources, J.B.; data curation, S.S.; writing–original draft preparation, S.S., M.A.K.; writing–review and editing, J.B., D.A.; visualization, S.S.; supervision, J.B., D.A.; project administration, J.B.; funding acquisition, J.B.. All authors have read and agreed to the published version of the manuscript.

Competing interests. No competing interests are present.

Acknowledgements. The present study is supported by UL Renewables and the Natural Science and Engineering Research Council of Canada (NSERC) through Alliance grant no. 556326. Computational resources provided by the Digital Research Alliance of Canada (www.alliancecan.ca) and Advanced Research Computing at the University of British Columbia (www.arc.ubc.ca) are gratefully acknowledged.

https://doi.org/10.5194/wes-2023-171
Preprint. Discussion started: 8 January 2024

eawe european academy of wind energy
Open Access WIND ENERGY SCIENCE DISCUSSIONS

References

Allaerts, D. and Meyers, J.: Boundary-layer development and gravity waves in conventionally neutral wind farms, Journal of Fluid Mechanics, 814, 95–130, https://doi.org/10.1017/jfm.2017.11, 2017.

Allaerts, D. and Meyers, J.: Gravity Waves and Wind-Farm Efficiency in Neutral and Stable Conditions, Boundary-Layer Meteorology, 166, https://doi.org/10.1007/s10546-017-0307-5, 2018.

Allaerts, D. and Meyers, J.: Sensitivity and feedback of wind-farm-induced gravity waves, Journal of Fluid Mechanics, 862, 990–1028, https://doi.org/10.1017/jfm.2018.969, 2019.

Bennett, A. F.: Open Boundary Conditions for Dispersive Waves, Journal of Atmospheric Sciences, 33, 176 – 182, https://doi.org/https://doi.org/10.1175/1520-0469(1976)033<0176:OBCFDW>2.0.CO;2, 1976.

Béland, M. and Warn, T.: The Radiation Condition for Transient Rossby Waves, Journal of Atmospheric Sciences, 32, 1873 – 1880, https://doi.org/https://doi.org/10.1175/1520-0469(1975)032<1873:TRCFTR>2.0.CO;2, 1975.

Centurelli, G., Vollmer, L., Schmidt, J., Dörenkämper, M., Schröder, M., Lukassen, L. J., and Peinke, J.: Evaluating Global Blockage engineering parametrizations with LES, Journal of Physics: Conference Series, 1934, 012 021, https://doi.org/10.1088/1742-6596/1934/1/012021, 2021.

Inoue, M., Matheou, G., and Teixeira, J.: LES of a Spatially Developing Atmospheric Boundary Layer: Application of a Fringe Method for the Stratocumulus to Shallow Cumulus Cloud Transition, Monthly Weather Review, 142, 3418 – 3424, https://doi.org/https://doi.org/10.1175/MWR-D-13-00400.1, 2014.

Jonkman, J., Butterfield, S., Musial, W., and Scott, G.: Definition of a 5MW Reference Wind Turbine for Offshore System Development, National Renewable Energy Laboratory (NREL), https://doi.org/10.2172/947422, 2009.

Klemp, J. and Lilly, D.: Numerical Simulation of Hydrostatic Mountain Waves, J. Atmos. Sci., 35, 78–107, https://doi.org/10.1175/1520-0469(1978)035<0078:NSOHMW>2.0.CO;2, 1978.

Lanzilao, L. and Meyers, J.: An Improved Fringe-Region Technique for the Representation of Gravity Waves in Large Eddy Simulation with Application to Wind Farms, Boundary-Layer Meteorology, https://doi.org/10.1007/s10546-022-00772-z, 2022a.

Lanzilao, L. and Meyers, J.: Effects of self-induced gravity waves on finite wind-farm operations using a large-eddy simulation framework, vol. 2265, https://doi.org/10.1088/1742-6596/2265/2/022043, 2022b.

Lanzilao, L. and Meyers, J.: A parametric large-eddy simulation study of wind-farm blockage and gravity waves in conventionally neutral boundary layers, 2023.

Lin, Y.-L.: Mesoscale Dynamics, Cambridge University Press, 2007.

Maas, O.: Large-eddy simulation of a 15 GW wind farm: Flow effects, energy budgets and comparison with wake models, Frontiers in Mechanical Engineering, 9, https://doi.org/10.3389/fmech.2023.1108180, 2023.

Nappo, C. J., ed.: An Introduction to Atmospheric Gravity Waves, vol. 102 of *International Geophysics*, Academic Press, https://doi.org/https://doi.org/10.1016/B978-0-12-385223-6.00014-8, 2012.

Rampanelli, G. and Zardi, D.: A Method to Determine the Capping Inversion of the Convective Boundary Layer, Journal of Applied Meteorology - J APPL METEOROL, 43, 925–933, https://doi.org/10.1175/1520-0450(2004)043<0925:AMTDTC>2.0.CO;2, 2004.

Smith, R.: The wind farm pressure field, Wind Energy Science Discussions, 2023, 1–14, https://doi.org/10.5194/wes-2023-56, 2023.

Smith, R. B.: Linear theory of stratified hydrostatic flow past an isolated mountain, Tellus, 32, 348–364, https://doi.org/https://doi.org/10.1111/j.2153-3490.1980.tb00962.x, 1980.

https://doi.org/10.5194/wes-2023-171
Preprint. Discussion started: 8 January 2024

Smith, R. B.: Interacting Mountain Waves and Boundary Layers, Journal of the Atmospheric Sciences, 64, 594 – 607, https://doi.org/10.1175/JAS3836.1, 2007.

Smith, R. B.: Gravity wave effects on wind farm efficiency, Wind Energy, 13, 449–458, https://doi.org/https://doi.org/10.1002/we.366, 2010.

Stipa, S., Ajay, A., Allaerts, D., and Brinkerhoff, J.: TOSCA - An Open-Source Finite-Volume LES Environment for Wind Farm Flows, Wind Energy Science, 2023a.

Stipa, S., Ajay, A., Allaerts, D., and Brinkerhoff, J.: The Multi-Scale Coupled Model: a New Framework Capturing Wind Farm-Atmosphere Interaction and Global Blockage Effects, Wind Energy Science Discussions, 2023, 1–44, https://doi.org/10.5194/wes-2023-75, 2023b.